CONVOLUTION INTEGRAL-BASED LINEARISATION OF HELICOPTER MULTIBODY DYNAMICS

R. M. Leitner
IABG mbH, Innovation Centre, Einsteinstrasse 20, 85521 Ottobrunn, Germany

Abstract

A new method for linearising nonlinear helicopter dynamics has been developed which can handle periodic dynamics with non-minimum phase or all-pass response due to control inputs. Rotor blades that are elastically hinged to the rotor hub have the property of forcing the rotor hub and the fuselage downward during a collective control step input. The subsequent downward motion is of short duration and corresponds in its behavior to an all-pass. In this paper, a method based on the convolution integral is shown to linearise the dynamics despite non-minimum phase behavior. The linearisation computes the stability and control matrices of the time-invariant state-space model, which is used for stability studies and linear control design. The linearisation method is verified by comparing the eigenvalues of the linear state-space model with the eigenvalues of the Floquet state transition matrix and additionally by comparing the step responses of the nonlinear and linear models. For this purpose, two rotor configurations (one standard and one coaxial) are trimmed and linearised based on a nonlinear multibody model. Both the multibody model and trimming using a multi-dimensional secant method are explained to better understand the complexity of linearising helicopter dynamics.

Keywords

Helicopter, Linearisation, Stability Analysis, Multibody Dynamics

1. INTRODUCTION

In contrast to the linearisation of fixed-wing aircraft, the linearisation of helicopters is more complicated. On the one hand, this is because of the forces and moments, which change in trimmed condition periodically over one rotor revolution, and on the other hand, because of the non-minimum phase of the helicopter dynamics, which becomes particularly apparent with step inputs.

Due to the flexible blade root in modern helicopters, a step in the rotor blade pitch leads to an instantaneous increase in lift on the rotor blade, which briefly pushes the rotor hub and fuselage downwards. This non-minimum phase or all-pass behaviour can be explained with a power twister from the gym. If the two ends are pushed upwards, the centre of the power twister is lowered due to the spring stiffness.

One way to overcome the all-pass problem in linearisation is to create a full-state linear state-space model using parameter estimation. Time-domain methods, like the Output Error Method described by [1], are suitable for this but have the disadvantage that the computation time can be quite long and in some cases, no satisfactory results are obtained. If the motion of the helicopter is periodic, it is possible to determine its stability in form of eigenvalues using the state transition matrix $\mathbf{\Phi}(T,0)$ with the time T for one rotor rotation and Floquet's theory, cf. [2]. The eigenvalues are obtained from the eigenvalues $\boldsymbol{\lambda}^\star$ of the transition matrix by applying Floquet transformation. For the j-th eigenvalue λ_j with $n = 0, 1, 2, ...$ this results in:

$$\lambda_j = \frac{1}{T}\left[ln|\boldsymbol{\lambda}_j^\star| + i\left(tan^{-1}\left(\frac{\mathrm{Im}(\boldsymbol{\lambda}_j^\star)}{\mathrm{Re}(\boldsymbol{\lambda}_j^\star)}\right) + 2n\pi\right)\right] \quad (1)$$

Since the eigenvalues are calculated based on the transition matrix, they are also applicable to non-minimum phase dynamics. Floquet's theory is suitable for investigating stability and, if necessary, conclusions about the stability matrix can be drawn. However, a linear time-invariant state space model including the stability and control matrix is useful for designing the linear control laws.

Therefore, a linearisation method for calculating the stability and control matrix must be found that applies to the periodic and non-minimum phase helicopter dynamics.

2. LINEARISATION METHOD

For the linearisation of helicopter dynamics, a new method for computing the stability and the control matrix was developed, see [3]. The method designated by the abbreviation SEAL (State Equation Approximation for Linearisation) is based on the linear state equation containing the convolution integral, cf. [4].

doi: 10.25967/570400

$$\dot{\boldsymbol{x}}(t) = \boldsymbol{A}\left(\boldsymbol{\Phi}(t-0)\boldsymbol{x}(0) + \int_0^t \boldsymbol{\Phi}(t-\tau)\boldsymbol{B}(\tau)\boldsymbol{u}(\tau)d\tau\right) + \boldsymbol{B}\boldsymbol{u}(t) \tag{2}$$

Since SEAL is a numerical method, assumptions have to be made to use the linear state equation for linearisation.

The first assumption refers to the time interval to be considered for linearisation. It is assumed that one revolution of the main rotor is sufficient to calculate the stability matrix $\boldsymbol{A}$ and control matrix $\boldsymbol{B}$. So the time interval to be considered corresponds to

$$T = 2\pi\dot{\psi}^{-1} \tag{3}$$

with the rotor speed $\dot{\psi}$. The second and most important assumption yields that the control vector $\boldsymbol{u}$ is constant over one rotor revolution and thus can be extracted from the convolution integral.

Both assumptions have an immediate effect on the state and control matrix, which are no longer constant in time. The second assumption changes the state equation to the State Equation Approximation for Linearisation (SEAL), which gave the method its name.

$$\dot{\boldsymbol{x}}(t) = \boldsymbol{A}(t)\boldsymbol{\Phi}(t-0)\boldsymbol{x}(0) + \left(\boldsymbol{A}(t)\int_0^t \boldsymbol{\Phi}(t-\tau)\boldsymbol{B}(\tau)d\tau + \boldsymbol{B}(t)\right)\boldsymbol{u}(0) \tag{4}$$

The basis for the computation of the stability and control matrix has been created. Subsequently, Equation (4) is partially derived by the initial state vector $\boldsymbol{x}(0)$ and the control vector $\boldsymbol{u}(0)$ to obtain the calculation rules for the stability and control matrix computation.

2.1. Stability Matrix

The partial derivation of the State Equation Approximation for Linearisation according to the initial state vector leads to

$$\frac{\partial\dot{\boldsymbol{x}}(t)}{\partial\boldsymbol{x}(0)} = \dot{\boldsymbol{\Phi}}(t-0) = \boldsymbol{A}(t)\boldsymbol{\Phi}(t-0). \tag{5}$$

Transforming the time step into its angle increment $\Delta\psi$ gives $\boldsymbol{A}(\psi_i)\boldsymbol{\Phi}(\psi_i - 0) = \dot{\boldsymbol{\Phi}}(\psi_i - 0)$ with $i = 1, 2, ...$ and $\psi_1 = 0$. The state matrix $\boldsymbol{A}$ at azimuth ψ_i corresponds to the ratio of $\dot{\boldsymbol{\Phi}}(\psi_i - 0)$ and $\boldsymbol{\Phi}(\psi_i - 0)$.

$$\boldsymbol{A}(\psi_i) = \dot{\boldsymbol{\Phi}}(\psi_i - 0)\boldsymbol{\Phi}(\psi_i - 0)^{-1} \tag{6}$$

The state transition matrix $\boldsymbol{\Phi}(\psi - 0)$ transfers the state $\boldsymbol{x}(0)$ from azimuth 0 to ψ. The inverse of the state transition matrix enables the reverse, i.e. the transition from azimuth ψ to 0. If the inverse is considered in Equation (2), the state vector $\boldsymbol{x}(\psi)$ is transferred to $\psi = 0$ so that the state vector for zero azimuth results. This is followed by multiplication with the time derivative of the state transition matrix $\dot{\boldsymbol{\Phi}}(\psi - 0)$, which allows the state $\boldsymbol{x}(0)$ to be converted to $\dot{\boldsymbol{x}}_x(\psi)$.

If the state matrix is azimuth-independent, a continuous time-invariant system exists. Finally, the time-invariant state matrix is formed as an arithmetic mean of azimuth-dependent state matrices over one rotor revolution, which corresponds to $N\Delta\psi$.

$$\bar{\boldsymbol{A}} = \frac{1}{N}\sum_{i=1}^{N}\boldsymbol{A}(\psi_i) \tag{7}$$

The azimuth vector reads

$$\boldsymbol{\psi} = \begin{bmatrix}\Delta\psi & 2\Delta\psi & ... & (N-1)\Delta\psi & N\Delta\psi\end{bmatrix}. \tag{8}$$

2.2. Control Matrix

The partial derivative by the control vector results in

$$\frac{\partial\dot{\boldsymbol{x}}(t)}{\partial\boldsymbol{u}(0)} = \dot{\boldsymbol{\Theta}}(t-0) = = \boldsymbol{A}(t)\int_0^t \boldsymbol{\Phi}(t-\tau)\boldsymbol{B}(\tau)d\tau + \boldsymbol{B}(t). \tag{9}$$

A closer look reveals that the integral of Equation (9) corresponds to the control transition matrix, which is labelled with $\boldsymbol{\Theta}$, that depends on the control vector $\boldsymbol{u}(0)$.

$$\int_0^t \boldsymbol{\Phi}(t-\tau)\boldsymbol{B}(\tau)d\tau = \frac{\partial\boldsymbol{x}(t)}{\partial\boldsymbol{u}(0)} = \boldsymbol{\Theta}(t-0) \tag{10}$$

Replacing the integral with the control transition matrix results in $\dot{\boldsymbol{\Theta}}(t-0) = \boldsymbol{A}(t)\boldsymbol{\Theta}(t-0) + \boldsymbol{B}(t)$.

A special case exists for $t = 0$. Then $\boldsymbol{\Theta}(t-0)$ becomes a null matrix and $\boldsymbol{B}(t)$ corresponds to $\dot{\boldsymbol{\Theta}}(t-0)$. The special case corresponds to a linearisation in one operating point. In case of an elastic main rotor this leads e.g. to a wrong sign of the vertical control derivative Z_{col} due to the all-pass behaviour of the vertical dynamics of the helicopter.

Analogous to the stability matrix the time-invariant control matrix is formed as an arithmetic mean over one revolution

$$\bar{\boldsymbol{B}} = \frac{1}{N}\sum_{i=1}^{N}\boldsymbol{B}(\psi_i) \tag{11}$$

with $\boldsymbol{B}(\psi_i) = \dot{\boldsymbol{\Theta}}(\psi_i - 0) - \boldsymbol{A}(\psi_i)\boldsymbol{\Theta}(\psi_i - 0)$.

With the matrices $\bar{\boldsymbol{A}}$ and $\bar{\boldsymbol{B}}$, the linear time-invariant state space model $\dot{\boldsymbol{x}}(t) = \bar{\boldsymbol{A}}\boldsymbol{x}(t) + \bar{\boldsymbol{B}}\boldsymbol{u}(t)$ of the helicopter dynamics can be obtained for a given flight condition, e.g. hovering flight.

3. HELICOPTER CONFIGURATIONS

Two helicopter configurations were selected for the verification of the linearisation method.

The first one represents a conventional helicopter with a main and a tail rotor (SMR-TR), and the second corresponds to a coaxial configuration (DMR-VO) where the fuselage is located between the two counterrotating main rotors.

Both configurations are available in reality and are based on the Trex 450 platform developed by the Asian manufacturer Align.

3.1. Single Main Rotor with Tail Rotor

The SMR-TR configuration represents a helicopter with one main and one tail rotor and corresponds to the typical design of a conventional helicopter. The helicopter is equipped with a three-bladed rotor head to improve smooth running. The landing gear gives the helicopter a secure stand even in rough terrain. The configuration is driven by a brushless electric motor.

Cyclic and collective control of the swashplate is provided by three electromechanical actuators installed in a Ypsilon arrangement around the main rotor shaft. The tail rotor pitch is driven by an actuator mounted close to the centre of gravity of the helicopter and is connected to the tail rotor pitch control mechanism by a thin stiff rod.

Figure 1 shows the CAD model of the SMR-TR configuration with two instead of the usual three tail rotor blades.

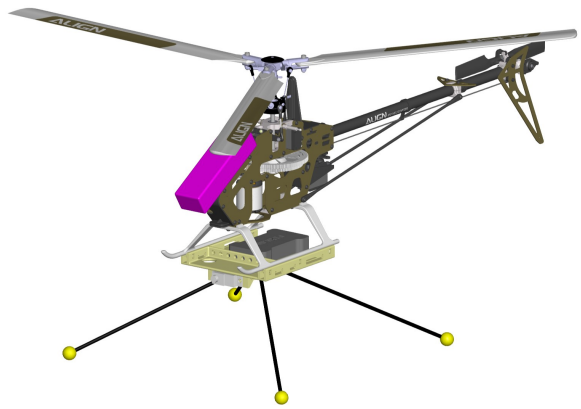

FIG 1. CAD Model of the SMR-TR Configuration

The key data of the SMR-TR configuration can be taken from Table 1.

TAB 1. Data of the SMR-TR Configuration

Description	Value	Unit
Total Mass	1026	g
Length without landing gear and rotors	600	mm
Diameter of the rotor	724	mm
Diameter of the tail rotor	164	mm
Height with landing gear	335	mm
Virtual flapping hinge offset of the rotor blade	37	mm
Chord length of the rotor blade	32	mm
Flapping moment of inertia of the rotor blade	0.88	gm^2
Lift curve slope of the rotor blade	5.59	1/rad
Operating speed of the rotor	2000	rpm
Spring stiffness of the rotor blade	0.5	Nm/rad
Damper constant of the rotor blade	0.01	Nms/rad
Lock number of the rotor blade	2.78	-

3.2. Double Main Rotor with Vertical Offset

DMR-VO denotes the coaxial helicopter configuration. There are two rotors in this configuration, which are vertically offset from each other and rotate in opposite directions. Figure 2 shows the CAD Model of the DMR-VO configuration.

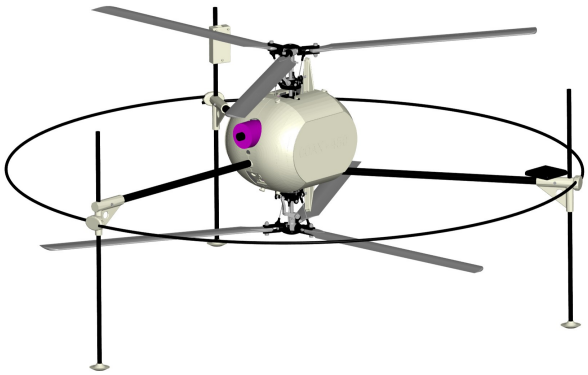

FIG 2. CAD Model of the DMR-VO Configuration - [5]

The fuselage is located in the middle of the two rotors and contains the rotor mechanics including the motor, gearbox and six electro-mechanical servos. The rotor mechanism corresponds to the SMR-TR mechanism, whereby this is in duplicate and mirrored to each other.

The longitudinal and lateral movement is done analogous to the SMR-TR configuration by tilting the swashplates longitudinally and laterally. The same applies to vertical movement. The yaw movement is generated by differential collective. Due to the mechanical arrangement of the two rotors, the landing gear has the shape of a tripod with arms protruding from the fuselage like spider legs.

The key data of the reference configuration are shown in Table 2.

TAB 2. Data of the DMR-VO Configuration

Description	Value	Unit
Total Mass	1154	g
Diameter of the rotor	724	mm
Height with landing gear	350	mm
Virtual flapping hinge offset of the rotor	37	mm
Chord length of the rotor blade	32	mm
Flapping moment of inertia of the rotor blade	0.88	gm^2
Lift curve slope of the rotor blade	5.59	1/rad
Operating speed of the rotor	2000	rpm
Spring stiffness of the rotor blade	0.5	Nm/rad
Damper constant of the rotor blade	0.01	Nms/rad
Lock number of the rotor blade	2.78	-

3.3. Helicopter Multibody Dynamics

Both helicopter configurations consist of a fuselage, two rotors with three rotor blades each and a landing gear composed of three or four landing legs. The topology of each helicopter model with respect to the Earth, which is assumed to be fixed and flat, is shown in Figure 3.

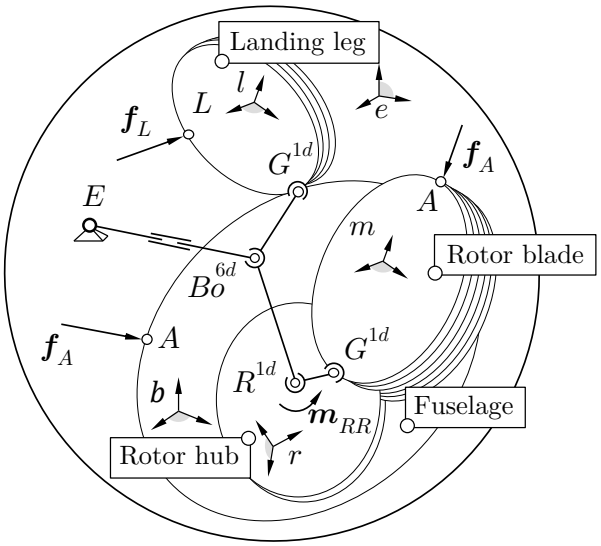

FIG 3. Topology of the helicopter models

The Earth (E, e) with reference point E and base e represents the inertial system in which the Equations of Motion of the helicopter models are developed.

The fuselage (Bo, b, B) is connected to the Earth by a 6-DOF hinge Bo^{6d}, which consists of three linear and three angular Degrees of Freedom. Four landing legs (L, l, L), which are coupled to the fuselage by a single hinge G^{1d}, allow interaction of the helicopter with the ground. The two rotor hubs (R, r, R), each equipped with a single-axis hinge R^{1d}, are rotatably mounted in the fuselage and are driven by an electric motor. Three rotor blades (M, m, M) are each connected by a single-axis hinge G^{1d} to the corresponding rotor hub to enable the flapping motion and to ensure horizontal propulsion of the helicopter by tilting the tip-path plane of the rotor longitudinally or laterally.

The Equations of Motion of the helicopter model are based on the principle of virtual velocity, also known as Jourdain's principle, see [6], which "couples" the Equations of Motion of the rigid bodies of the helicopter multibody model, see Equation (12), with Jacobi matrices $\boldsymbol{J}_\eta$ and $\boldsymbol{J}_q$ that implicitly contain the helicopter linear and angular Degrees of Freedom.

$$\boldsymbol{M}\dot{\boldsymbol{\eta}} = \boldsymbol{J}_\eta^\top \left[\boldsymbol{e} - \boldsymbol{j} - \boldsymbol{g}\right] \tag{12}$$

The term $\boldsymbol{M} = \boldsymbol{J}_\eta^\top \boldsymbol{M}^\star \boldsymbol{J}_\eta$ represents the mass matrix. The generalised forces and moments correspond to the product of the transposed Jacobian $\boldsymbol{J}_\eta^\top$ and the force and moment vector $\boldsymbol{e}$. The variable $\boldsymbol{j}$ is equivalent to $\boldsymbol{M}^\star \boldsymbol{J}_q \boldsymbol{\eta}$.

In the multibody model of the helicopter, 13 rigid bodies are geometrically coupled using ideal hinges and bearings, so that the model exhibits 18 Degrees of Freedom (DOF) or minimal coordinates.

Detailed information on the multibody dynamics of the two helicopter models can be found in [3].

3.4. Trimming

Figures 4 and 5 show the two helicopter configurations in trimmed hover flight, which have been computed with a trim program based on the multidimensional secant method.

$$\boldsymbol{p}^{k+1} = \boldsymbol{p}^k + \left[\frac{\partial \dot{\tilde{\boldsymbol{x}}}^k}{\partial \boldsymbol{p}^k}\right]^{-1} \left[\dot{\tilde{\boldsymbol{x}}}_{des} - \dot{\tilde{\boldsymbol{x}}}^k\right] \tag{13}$$

The vector $\boldsymbol{p}$, which combines the variable parameters of the state and control vector, is modified by the trim programme at each step k of the iteration.

The iteration stops if the state derivatives $\dot{\tilde{\boldsymbol{x}}}^k$ gets sufficiently close to the desired state derivatives $\dot{\tilde{\boldsymbol{x}}}_{des}$, which define the trim case. The stop criterion is fulfilled if the inequality

$$\left|\left|\boldsymbol{S}\left[\dot{\boldsymbol{x}}_{des} - \dot{\boldsymbol{x}}^k\right]\right|\right|_2^2 = \left|\left|\left[\dot{\tilde{\boldsymbol{x}}}_{des} - \dot{\tilde{\boldsymbol{x}}}^k\right]\right|\right|_2^2 < \epsilon \tag{14}$$

is met. Here ϵ represents a lower limit that is set before the trimming process starts and ensures that the iteration is aborted if the lower limit is undershot. Matrix $\boldsymbol{S}$ acts as a selection matrix, which separates the trim-specific residuals from the residual vector to form the cost function.

The vector $\boldsymbol{p}$ involves the roll ϕ_{bg} and pitch angle θ_{bg} of the fuselage, the turn rates $\dot{\psi}$ of both rotors, the flapping angles β' and rates $\dot{\beta}'$ of all six rotor blades, the four landing leg deflections ϕ and rates $\dot{\phi}$ as well as the two induced velocities w of the uniformly

distributed rotor flow models.

Fixed values with which the flight condition can be set are, in addition to the height of the helicopter above ground $h_{EBo,e}$, the rotational speeds of the rotors $\dot{\psi}$, the fuselage-fixed rotation rates $p^g_{b,b}$, $q^g_{b,b}$ and $r^g_{b,b}$ as well as the vertical positions $z_{BoR,b}$ of the rotors.

$\phi_{bg} = 3.3569°$, $\theta_{bg} = -0.0863°$, $h_{EBo,e} = 1.0000$ m,
$\beta^2_0 = 1.0874°, \beta^2_{1c} = -0.0619°, \beta^2_{1s} = -0.0620°$

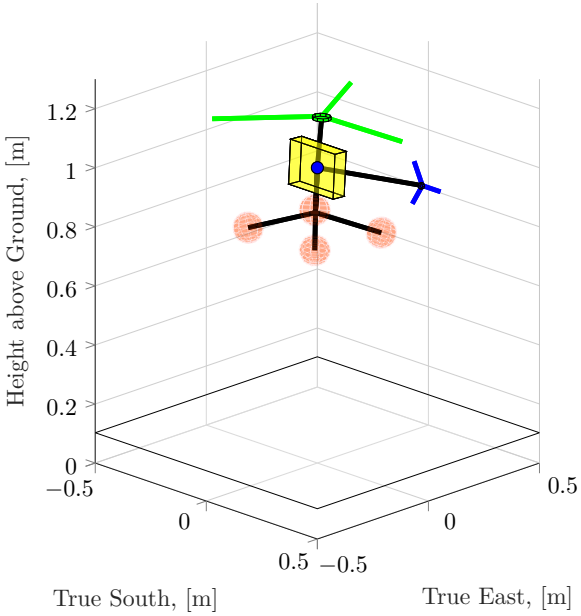

FIG 4. SMR-TR configuration in Hover Flight

$\phi_{bg} = -0.0236°$, $\theta_{bg} = -0.2137°$, $h_{EBo,e} = 1.0000$ m,
$\beta^2_0 = 0.7361°, \beta^2_{1c} = -0.1539°, \beta^2_{1s} = -0.0622°$

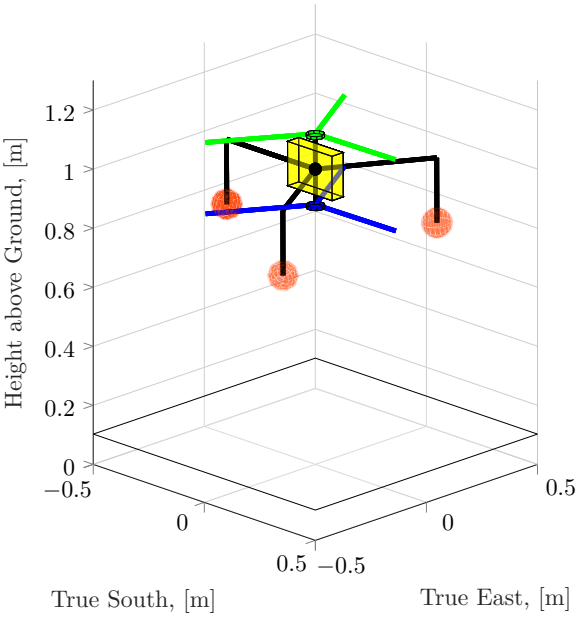

FIG 5. DMR-VO configuration in Hover Flight

If the helicopter dynamics are simulated with the trim states as initial values of the integrators over a time of three rotor revolutions, different time courses result, see Figures 6 and 7.

The courses are periodic and some of them drift away slightly. The drifts are due to the trim strategy, which neglects the periodicity of the fuselage states: $u^{E,e}_{Bo,b}$, $v^{E,e}_{Bo,b}$, $w^{E,e}_{Bo,b}$, $p^g_{b,b}$, $q^g_{b,b}$ and $r^g_{b,b}$.

For the trim and stability analysis, the drifts are negligible as their influence on the results is small.

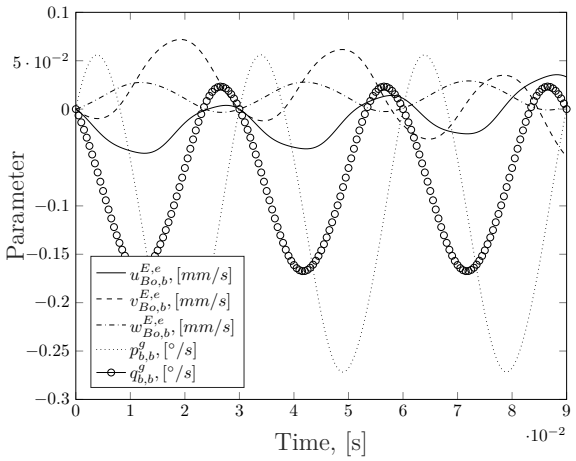

FIG 6. SMR-TR States over three Rotor Revolutions

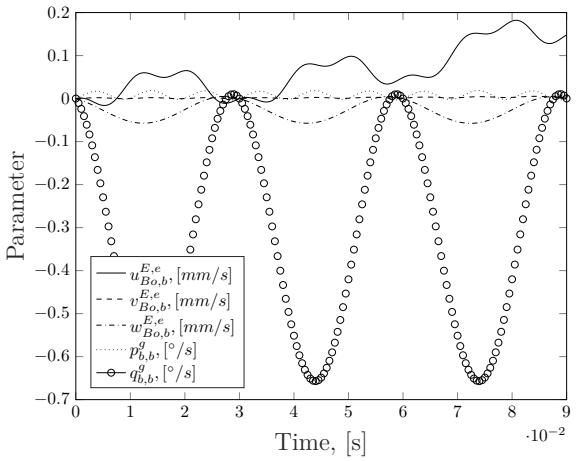

FIG 7. DMR-VO States over three Rotor Revolutions

Detailed information on trim can be found in [3].

4. LINEARISATION RESULTS

In order to verify the suitability of the SEAL method for the linearisation of non-minimum phase helicopter dynamics, three verification tests are carried out in the following.

4.1. Eigenvalues

A comparison of the Floquet and SEAL eigenvalues is carried out to ensure that the new linearisation method computes correctly.

The SMR-TR eigenvalues derived from the Floquet State Transition Matrix (FSTM) and SEAL. The SEAL eigenvalues are computed for different numbers of azimuth positions N of the main rotor. It is noticeable that with increasing N, the difference between FSTM and SEAL decreases, see Table 3.

TAB 3. Eigenvalues of SMR-TR in Hover Flight

FSTM	SEAL (N = 10)	SEAL (N = 100)
$-14.9200 \pm 6.3868i$	$-15.8439 \pm 7.2945i$	$-14.8686 \pm 6.3391i$
rel. error in %	$+ 6.1924 + 14.2121i$	$- 0.3445 - 0.7469i$
$+ 0.0254 \pm 1.1065i$	$+ 0.0217 \pm 1.1016i$	$+ 0.0257 \pm 1.1068i$
rel. error in %	$-14.5669 - 0.4428i$	$+ 1.1811 + 0.0271i$
$- 2.2983$	$- 2.3118$	$- 2.2970$
rel. error in %	$+ 0.5874$	$- 0.0566$
$- 1.5573$	$- 1.7106$	$- 1.5678$
rel. error in %	$+ 9.8440$	$+ 0.6742$
$- 1.1757$	$- 0.9374$	$- 1.1700$
rel. error in %	-20.2688	$- 0.4848$
$+ 0.1866$	$+ 0.1191$	$+ 0.1874$
rel. error in %	-36.1736	$+ 0.4287$

4.2. Linearised versus Multibody Dynamics

A comparison of the two models using numerical simulation shows how well the averaged results of the SEAL method agree with the nonlinear multibody model. For this purpose, the linear (lin.) dynamics with $N = 100$ and the nonlinear (non-lin.) multibody dynamics are stimulated with equal step inputs and simulated for a time of 1.5 seconds, see Figures 8 and 9. The starting point of the simulation is the trimmed hover flight, which is stimulated by a multi-axis step input with $\Delta\delta_{lon} = -\Delta\delta_{lat} = -\Delta\delta_{col} = 0.1°$.

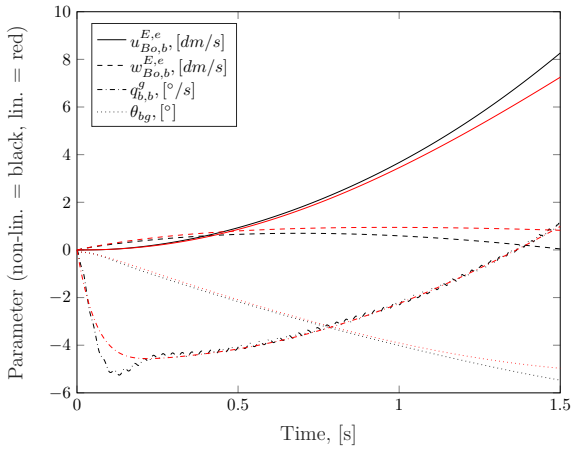

FIG 8. Longitudinal Responses of SMR-TR

As can be seen in Figures 8 and 9, both models show relatively good agreement. The linear model is an averaging of the nonlinear multibody dynamics, which are strongly influenced by the high-frequent rotor blade motions, see the states $q^g_{b,b}$ and $p^g_{b,b}$. Therefore, the overshoot in the $q^g_{b,b}$ graph of the nonlinear model that occurs in the time interval between 0 and 0.25 seconds in Figure 8 is not observed in the graph of the linear model. Furthermore, it can be seen that the time courses diverge towards the end of the simulation time, which is due to the strongly nonlinear

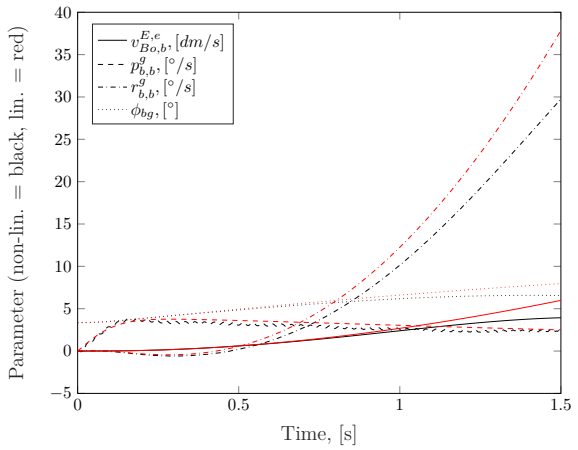

FIG 9. Lateral Responses of SMR-TR

dynamics of the multibody model, which the linear model is not able to follow.

Figures 10 and 11 show the open-loop step responses of the linear (lin.) and nonlinear (non-lin.) models of the DMR-VO configuration due to the same multi-axis step input as used for SMR-TR configuration. The simulation time is 1.5 seconds.

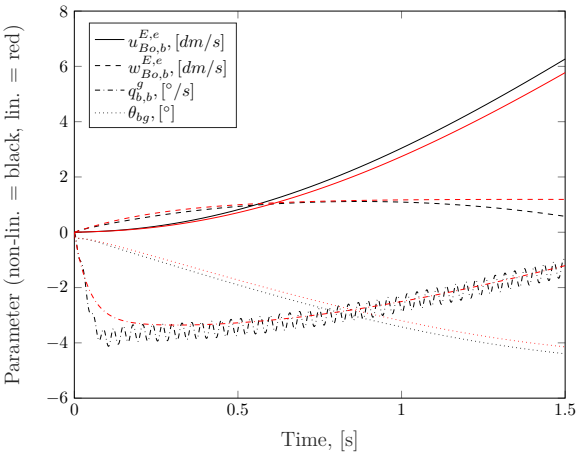

FIG 10. Longitudinal Responses of DMR-VO

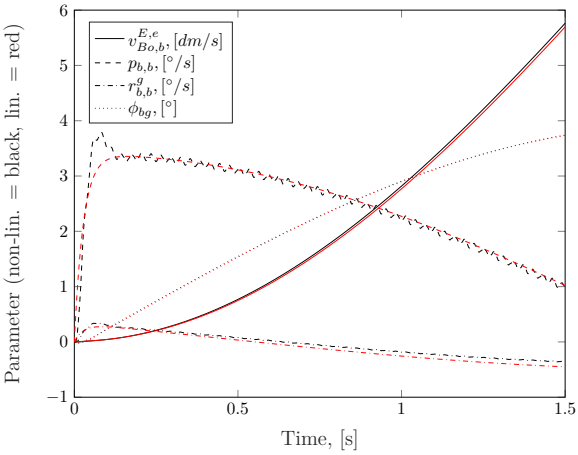

FIG 11. Lateral Responses of DMR-VO

Similar to the SMR-TR configuration, the graphs of the nonlinear and linear models of the DMR-VO configuration match relatively well. The overshoot of the $q^g_{b,b}$ graph is not present in the linear model. Since the DMR-VO configuration is roughly symmetric in structure, it is obvious that the roll rate of Figure 11 exhibits an overshoot similar to the pitch rate of Figure 10. Analogous to the SMR-TR configuration, the states $q^g_{b,b}$ and $p^g_{b,b}$ oscillate due to the high-frequent blade motion.

4.3. Hovering Cubic

The third and final verification test on the static and dynamic stability of the helicopter in hover flight shows how well the SEAL method copes with parameter changes in the simulation model.

Conventional helicopters like the SMR-TR configuration are statically stable but exhibit dynamic instability when hovering. Responsible for this is the positive speed stability M_u, whose magnitude and sign depends significantly on the vertical distance of the main rotor Neutral Point with respect to the helicopter's centre of gravity B. A helicopter whose Neutral Point is below its centre of gravity exhibits dynamic stability and static instability due to a negative M_u.

The Neutral Point is located in, above or below the rotor hub R. The exact position h depends essentially on the flapping hinge offset a and the coning angle β_0, see [3] and [7].

$$h = \frac{a}{2\beta_0} \tag{15}$$

If a is zero, the Neutral Point lies in the rotor hub. If not, the Neutral Point is located above or below the hub, depending on the sign of the hinge offset.

For a better understanding of the influence of the Neutral Point position on stability, it is worth taking a look at the linearised equations of the longitudinal motion.

$$\begin{bmatrix} s - X_u & g - X_q s - X_\theta \\ -M_u & s^2 - M_q s - M_\theta \end{bmatrix} \begin{bmatrix} u \\ \theta \end{bmatrix} = \begin{bmatrix} X_{\delta_{lon}} \\ M_{\delta_{lon}} \end{bmatrix} \delta_{lon} \tag{16}$$

From these, the characteristic equation, also known as the Hovering Cubic (HC), can be derived.

$$\begin{aligned} HC = s^3 - (X_u + M_q)s^2 + (X_u M_q - M_u X_q - M_\theta)s + \\ + X_u M_\theta + M_u (g - X_\theta) = 0 \end{aligned} \tag{17}$$

The Hovering Cubic provides information on whether the longitudinal eigenmotion of the helicopter shows e.g. oscillations or a purely divergent behaviour. This depends mainly on the speed stability M_u, which is helicopter specific. Figure 12 shows the effect of M_u on the stability of the Hovering Cubic, cf. [8]. Note that $X_u < 0$, $M_q < 0$ and $\frac{\partial X_u}{\partial M_u} = \frac{\partial M_q}{\partial M_u} = 0$.

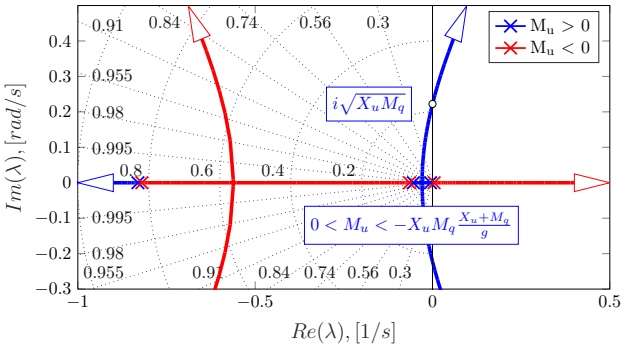

FIG 12. Effect of M_u on the stability of the HC

The blue coloured root locus of Figure 12 apply to helicopter configurations with positive M_u and the red to configurations with negative M_u values. The purely aperiodic blue coloured roots, which represents the Pitch Subsidence, lies in the left-hand side of the complex plane and thus represents a stable eigenmotion. The Phugoid, see the blue arc, is unstable for high M_u values. If the Neutral Point moves closer to the helicopter's centre of gravity, the Phugoid becomes stable and splits into two aperiodic eigenmotions. The transition from an unstable to a stable Phugoid to a stable aperiodic eigenmotion occurs in the M_u range of

$$0 < M_u < -X_u M_q \frac{X_u + M_q}{g}, \tag{18}$$

cf. [9]. If the Neutral Point is lowered further below the centre of gravity the right eigenmotion changes to the right half-plane. The aperiodic instability of this eigenmotion is caused by the static instability due to negative M_u values and causes a "Pitch Dive". The left eigenmotion merges with the roots of the Pitch Subsidence to form a stable oscillation mode.

The poles of the DMR-VO configuration are located on the blue root locus of Figure 12 and would change to the red root locus if the rotors were lowered below the centre of gravity.

A trimming calculation with subsequent linearisation for different vertical rotor distances to the centre of gravity of the multibody helicopter dynamics shows that the pole wandering matches the root locus of Figure 12 relatively well, see Figure 13.

The only difference between the two figures is the curvature of the red root locus on the left side of the complex plane. While the root locus in Figure 12 turns to the left, it turns to the right in Figure 13. This is because the root locus in Figure 12 has been calculated with constant M_q. Since the pitch damping decreases

with the vertical lowering of the rotors $z_{BR,b}$, see Figure 14, this changes the curvature to the right.

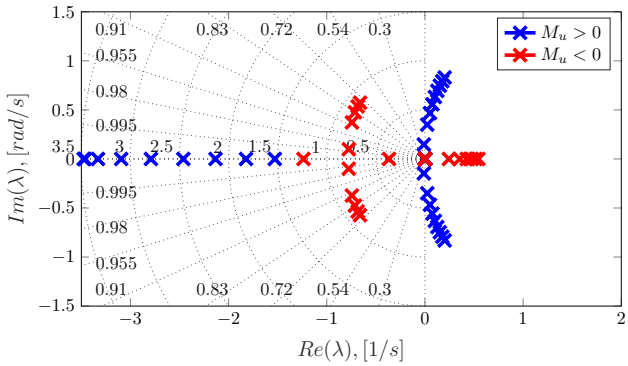

FIG 13. Pole wandering with variation of the averaged vertical rotor distance $z_{BR,b}$

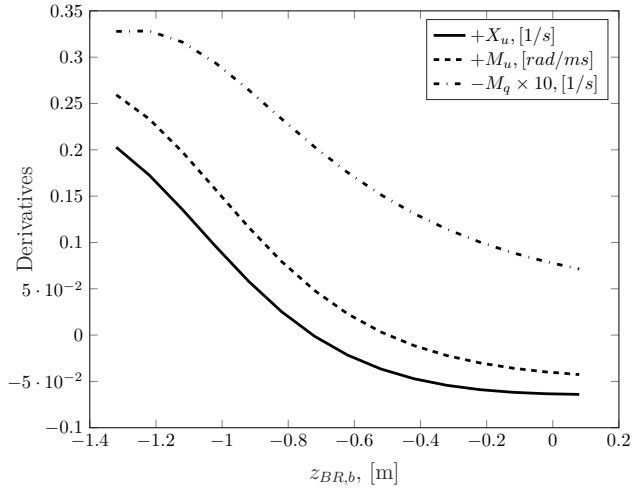

FIG 14. Course of the derivatives with variation of the averaged vertical rotor distance $z_{BR,b}$

5. CONCLUSIONS AND OUTLOOK

Within the scope of this paper, a numerical method for the linearisation of nonlinear multibody helicopter dynamics was presented, which can handle non-minimum phase helicopter dynamics due to elastic blade hinges. The algorithm, which is abbreviated SEAL and stands for State Equation Approximation for Linearisation, is based on the convolution integral and provides the linear time-invariant state and control matrix of the helicopter dynamics as a result. The operating point for the linearisation is the periodically trimmed helicopter dynamics.

The suitability of the SEAL method for linearising the multibody dynamics of helicopters with different rotor configurations was demonstrated by various verification tests. These include a comparison of the SEAL eigenvalues with the eigenvalues calculated using Floquet theory which is based on the transition matrix for one rotor revolution. Another test compared the step responses of the linear time-invariant dynamics with the nonlinear dynamics of the multibody model to show how well the averaged results of the SEAL method agree with the nonlinear multibody model. In a final test, the linearisation results for different velocity derivatives were compared with the stability theory derived from the hovering cubic. This involved moving the rotor hubs of a coaxial configuration along the vertical axis of the rotors above or below the centre of gravity of the helicopter, which had a stabilising or destabilising effect on the helicopter dynamics.

The results of the verification tests confirm the correctness of the SEAL method, so that stability analyses for different parameter variations, e.g. various kinematic velocities, or additional rigid bodies, e.g. slung load, can be carried out. Furthermore, it will be investigated whether the SEAL method can also be applied to other, more complex structured rotor inflow models.

Contact address:

roland.leitner@iabg.de

References

[1] R. V. Jategaonkar. *Flight Vehicle System Identification: A Time Domain Method*. American Institute of Aeronautics and Astronautics, Inc., 2006.

[2] D. A. Peters and K. H. Hohenemser. Application of the Floquet Transition Matrix to Problems of Lifting Rotor Stability. *Journal of the American Helicopter Society*, 1970.

[3] R. M. Leitner. *Modelling and Verification of Helicopter Multibody Dynamics for different Rotor Configurations*. PhD thesis, RWTH Aachen, 2022.

[4] G. Ludyk. *Theoretische Regelungstechnik 1*. Springer-Verlag Berlin Heidelberg, 1995.

[5] D. Kreuzpaintner. Entwicklung, Konstruktion und Bau eines Koaxialhubschraubers. Master's thesis, Munich University of Applied Sciences, 2015.

[6] P. E. B. Jourdain. Note on an analogue of gauss principle of least constraint. *Q. J. Pure Appl. Math. 8L*, page 153157, 1909.

[7] W. Just. *Hubschrauber und Vertikalstartflugzeuge*. Verlag Flugtechnik Stuttgart, 1962.

[8] H. T. Albachten and G. J. Sissingh. Stability Analyses of Flying Platform in Hovering and Forward Flight. Technical report, Advanced Research Division of Hiller Helicopters, 1956.

[9] X. Hafer and G. Sachs. *Senkrechtstarttechnik*. Springer-Verlag, 1982.